Author(s): Schatte, Gabriele; Chivers, Tristram; Tuononen, Heikki; Suontamo, Reijo; Laitinen, Risto; Valkonen, Jussi

Title: Experimental and Theoretical Investigations of Tellurium(IV) Diimides and Imidotelluroxanes: X-ray Structures of B(C6F5)3 Adducts of OTe(μ-NtBu)2TeNtBu, [OTe(μ-NtBu)2Te(μ-O)]2 and tBuNH2

Year: 2005

Version:

Please cite the original version:

Schatte, G., Chivers, T., Tuononen, H., Suontamo, R., Laitinen, R., & Valkonen, J. (2005). Experimental and Theoretical Investigations of Tellurium(IV) Diimides and Imidotelluroxanes: X-ray Structures of B(C6F5)3 Adducts of OTe(μ-NtBu)2TeNtBu, [OTe(μ-NtBu)2Te(μ-O)]2 and tBuNH2. Inorganic Chemistry, 44(2), 443-451. https://doi.org/10.1021/ic048565+

Experimental and Theoretical Investigations of Tellurium(IV) Diimides and Imidotelluroxanes: X-ray Structures of $B(C_6F_5)_3$ adducts of $OTe(\mu\text{-}N^tBu)_2TeN^tBu$, $[OTe(\mu\text{-}N^tBu)_2Te(\mu\text{-}O)]_2$ and $^tBuNH_2$

Gabriele Schatte, [†] Tristram Chivers,*[,†] Heikki M. Tuononen, [‡] Reijo Suontamo, [‡] Risto Laitinen[§] and Jussi Valkonen[‡]

Departments of Chemistry, University of Calgary, 2500 University Drive N. W., Calgary, Alberta, Canada T2N 1N4, University of Jyväskylä, P. O. Box 35, FIN-40014 Jyväskylä, Finland, and University of Oulu, P. O. Box 3000, FIN-90014 Oulu, Finland

---

* To whom correspondence should be addressed.

E-mail: chivers@ucalgary.ca. Telephone: (403) 220-5741. Fax: (403) 289-9488.

† University of Calgary

‡ University of Jyväskylä

§ University of Oulu

Abstract

The hydrolysis of ^{t}BuNTe(μ-N^{t}Bu)$_2$TeN^{t}Bu (**1**) with one or two equivalents of $(C_6F_5)_3B\cdot H_2O$ results in the successive replacement of terminal imido groups by oxo ligands to give the telluroxane-Lewis acid adducts $(C_6F_5)_3B\cdot$OTe(μ-N^{t}Bu)$_2$TeN^{t}Bu (**2**) and [$(C_6F_5)_3B\cdot$OTe(μ-N^{t}Bu)$_2$Te(μ-O)]$_2$ (**3**), which were characterized by multinuclear NMR spectroscopy and by X-ray crystallography. The Te=O distance in **2** is 1.870(2) Å. The di-adduct **3** involves the association of four ^{t}BuNTeO monomers to give a tetramer in which both terminal Te=O groups [d(TeO) = 1.866(3) Å] are coordinated to $B(C_6F_5)_3$. The central Te_2O_2 ring in **3** is distinctly unsymmetrical [d(TeO) = 1.912(3) and 2.088(2) Å]. The X-ray structure of $(C_6F_5)_3B\cdot NH_2{}^{t}$Bu (**4**), the by-product of these hydrolysis reactions, is also reported. The geometries and energies of tellurium(IV) diimides and imido telluroxanes were determined by using quantum chemical calculations. The calculated energies for the reactions $E(NR)_2$ + $Te(NR)_2$ (E = S, Se, Te; R = H, Me, ^{t}Bu, $SiMe_3$) confirm that cyclodimerization of tellurium(IV) diimides is strongly exothermic. In the mixed chalcogen systems, the cycloaddition is energetically favorable for the Se/Te combination. The calculated energies for the further oligomerization of the dimers XE(μ-NMe)$_2$EX (E = Se, Te; X = NMe, O) indicate that the formation of tetramers is strongly exothermic for the tellurium systems, but endothermic (X = NMe) or thermoneutral (X = O) for the selenium systems, consistent with experimental observations.

Introduction

The structures of chalcogen dioxides EO_2 (E = S, Se, Te) reflect the increasing reluctance of the heavier chalcogens to engage in multiple bonding with oxygen (Scheme 1). Sulfur dioxide is monomeric in the gas phase (microwave spectroscopy)[1a] and in the solid state (low temperature X-ray diffraction study)[1b]. By contrast, selenium dioxide is a two-dimensional polymer in the solid state with both single and double SeO bonds[2-4] and tellurium dioxide is a three-dimensional polymer with only single TeO bonds.[5] The dimer *trans*-OSe(μ-O)$_2$SeO has been identified in the vapor of SeO_2 by a matrix IR study.[6] The trend towards polymeric structures is less pronounced for the isoelectronic chalcogen diimides $E(NR)_2$, presumably as a result of the combination of less polar bonds and the steric influence of the substituent attached to the nitrogen atoms. While both sulfur and selenium diimides are monomeric,[7,8] the known tellurium diimides form dimers of the type RNTe(μ-N^{t}Bu)$_2$TeNR (R = ^{t}Bu, PPh_2NSiMe_3) in the solid state.[9-11] Hybrid imido-oxo systems of the type OENR are monomeric for E = S both in the solid state[13] and in the gas phase.[12] However, the only structurally characterized selenium analogue OSe(μ-N^{t}Bu)$_2$SeO is dimeric in the solid state.[8] This article describes experimental and theoretical investigations of the previously unknown imidotelluroxanes $(OTeNR)_n$ (R = H, Me, ^{t}Bu, $SiMe_3$).

Insert Scheme 1 here.

Thionylimines RNSO and their selenium analogues, e.g., ^{t}BuNSeO, are typically prepared by the reaction of a primary amine, or the trimethylsilylated derivative, with $OSCl_2$ or $OSeCl_2$, respectively.[12,14] Since the corresponding tellurium reagent $OTeCl_2$ is not readily available, an alternative synthetic strategy had to be developed for the preparation of imidotelluroxanes. We report here the generation of these hybrid imido-oxo systems by the controlled hydrolysis of the tellurium diimide dimer ^{t}BuNTe(μ-N^{t}Bu)$_2$TeN^{t}Bu (**1**) using the hydrate $(C_6F_5)_3B{\cdot}H_2O$[15] as a stoichiometric

reagent. This approach allows the successive replacement of terminal N^{t}Bu groups by oxo ligands to give the imidotelluroxanes OTe(μ-N^{t}Bu)$_2$TeN^{t}Bu and [OTe(μ-N^{t}Bu)$_2$Te(μ-O)]$_2$ as the Lewis acid adducts **2** and **3**, respectively (see Scheme 2). The X-ray structures of **2** and **3** and of $(C_6F_5)_3B{\cdot}NH_2{}^tBu$ (**4**), the by-product of these hydrolysis reactions, are discussed. The hydrate $(C_6F_5)_3B{\cdot}H_2O$ has previously been employed by Roesky and co-workers for the preparation of the monoalumoxane $LAlO{\cdot}B(C_6F_5)_3$ by the stoichiometric hydrolysis of $LAlMe_2$ (L = $Et_2NCH_2CH_2C(Me)CHC(Me)NCH_2CH_2NEt_2$).[16] Quantum chemical calculations of the geometries and energies of tellurium(IV) diimides and imidiotelluroxanes using quasi-relativistic effective core potential (ECP) basis sets have been carried out. The cycloaddition energies for the reactions $E(NR)_2$ + $Te(NR)_2$ (E = S, Se, Te; R = H, Me, ^{t}Bu, $SiMe_3$) and for the cyclooligomerization of the dimers XE(μ-NMe)$_2$EX (E = Se, Te; X = NMe, O) have also been calculated for comparison with experimental observations.

Experimental Section

Reagents and General Procedures. Solvents were dried and distilled over Na/benzophenone (tetrahydrofuran, toluene), sodium (*n*-pentane) or P_4O_{10} (dichloromethane). Deuterated solvents were dried over molecular sieves (3 Å) prior to use. The reagents *tert*-butylamine (Aldrich, 98%) and tris(pentafluorophenyl)borane (Boulder Scientific) were used as received. The starting materials ^{t}BuNTe(μ-N^{t}Bu)$_2$N^{t}Bu (**1**)[17] and $(C_6F_5)_3B{\cdot}OH_2$[15] were prepared according to literature procedure. All manipulations were performed under an argon atmosphere using standard Schlenk techniques or a glove box.

Instrumentation. ^{1}H, ^{11}B, ^{13}C and ^{125}Te NMR spectra were recorded on a Bruker DRX400 NMR spectrometer at 25 °C in C_4D_8O using a 5 mm broadband probe (BBO) operating at 399.873, 128.293, 100.559 and 126.349 MHz, respectively. Relaxation delays of 3 and 1.5 s were applied when measuring the ^{13}C{^{1}H} and ^{125}Te spectra, respectively. Line-broadening parameters used in the exponential

multiplication of the free induction decays, were 10 to 1 Hz. The samples for ^{125}Te NMR were externally referenced to K_2TeO_3 in D_2O and referred to Me_2Te. ^{1}H NMR chemical shifts are reported relative to Me_4Si in $CDCl_3$, ^{11}B NMR chemical shifts were externally referenced to $BF_3{\cdot}Et_2O$ in C_6D_6. ^{19}F NMR data were measured on a Bruker AMX300 NMR spectrometer at 25 °C in C_4D_8O using a 5 mm dual probe operating at 282.371 MHz, chemical shifts are reported relative to $CFCl_3$ and were measured with an external standard of C_6F_6 in the appropriate deuterated solvents (δ, −163 ppm). Infrared spectra were obtained as Nujol mulls between KBr plates on a Nicolet Nexus 470 FT-IR spectrometer in the 4000-350 cm^{-1} region (32 scans; resolution, 2 cm^{-1}). Elemental analyses were provided by the Analytical Services Laboratory, Department of Chemistry, University of Calgary.

Preparation of [$(C_6F_5)_3B{\cdot}OTe(\mu$-N^{t}Bu)$_2$TeN^{t}Bu] (2). A colorless solution of $(C_6F_5)_3B{\cdot}OH_2$ (0.294 g, 0.555 mmol) in CH_2Cl_2 (10 mL) was added to an orange-red solution of freshly sublimed **1** (0.300 g, 0.556 mmol) in *n*-pentane (20 mL) at −78 °C. The yellow-orange solution was allowed to reach 23 °C after 10 min and stirred for a further 2.5 h. The volatile materials were removed under vacuum to give **2** as a yellow-orange solid (0.454 g, 0.456 mmol; 82%). The product is very soluble in CH_2Cl_2, less soluble in toluene and insoluble in *n*-pentane. Yellow-orange rod-like crystals were obtained from a CH_2Cl_2 solution after 4 d at −20 °C. Anal. Calcd. for $C_{30}H_{27}BF_{15}N_3OTe_2$: C, 36.16; H, 2.73; N, 4.22. Found: C, 35.17; H, 2.93; N, 4.42. ^{1}H, ^{13}C and ^{19}F NMR spectra indicated the presence of two isomers **2a** and **2b** in solution: ^{1}H NMR (in CD_2Cl_2), δ 1.51 (9 H, ^{t}Bu), 1.37 (18 H, ^{t}Bu) (**2a**), 1.50 (9 H, ^{t}Bu), 1.28 (18 H, ^{t}Bu) (**2b**); ^{11}B NMR, δ −2.8; ^{13}C NMR, δ 149.4 (m, *para*) (**2a**), 147.0 (m, *para*) (**2b**), 141.2 (m, *ortho*) (**2a**), 138.7 (m, br, *meta*) (overlap of **2a** and **2b**), 136.4 (m, *ortho*) (**2b**), 123.2 (br, *ipso*) (overlap of **2a** and **2b**), 69.7, 59.6 (*C*Me$_3$) (**2a**), 68.8, 60.2 (*C*Me$_3$) (**2b**), 35.7, 35.2 (C*Me*$_3$) (**2b**), 35.5, 34.4 (C*Me*$_3$) (**2a**); ^{19}F NMR, δ −132.5 (m, *ortho*) (**2a**), −133.3 (m, *ortho*) (**2b**), −159.8 (m, *para*) (**2b**), −160.1 (m, *para*) (**2a**), −164.9 (m, *meta*) (**2b**), −165.2 (m, *meta*) (**2a)**; ^{125}Te NMR, δ□1384, 857; NMR data (in C_7D_8): ^{1}H NMR, δ 1.25 (9 H, ^{t}Bu), 0.86 (18 H, ^{t}Bu) (**A**), 1.42 (9 H, ^{t}Bu), 0.87 (18 H, ^{t}Bu) (**2b**);

^{11}B NMR, δ –2.6; ^{13}C NMR, δ 68.7, 59.0 (*C*Me$_3$) (**2a**), 69.4, 58.6 (*C*Me$_3$) (**2b**), {34.6, 34.0 (C*Me*$_3$) (**2b**), 34.3, 32.7 (C*Me*$_3$) (**2a**), the carbon shifts for the C_6F_5 groups were not observed owing to the low concentration. IR (cm^{-1}): 687 (Te=O).

Preparation of [(C$_6$F$_5$)$_3$B·OTe(*μ*-N^{t}Bu)$_2$Te(*μ*-O)]$_2$ (3). A colorless solution of $(C_6F_5)_3B{\cdot}OH_2$ (0.160 g, 0.301 mmol) in CH_2Cl_2 (10 mL) was added to an orange solution of **2** (0.300 g, 0.301 mmol) in CH_2Cl_2 (20 mL) at −78 °C. The yellow-orange solution was allowed to reach 23 °C very slowly. After 2 h the solution was filtered through a PTFE syringe filter disk (pore size, 0.45 μm) to remove trace amounts of tellurium. The volatile materials were removed under vacuum to give a sticky yellow-orange solid. The addition of toluene (5 mL) produced a pale yellow solid and an orange solution. The solution was decanted *via* a cannula and the pale yellow solid was pumped to dryness and identified as **3** (0.216 g, 0.115 mmol, 76%) by multinuclear NMR and IR spectroscopy. The product is insoluble in CH_2Cl_2, CH_3CN and in toluene, but soluble in THF. Anal. Calcd. for $C_{52}H_{36}B_2F_{30}N_4O_4Te_4$: C, 33.17; H, 1.93; N, 2.97. Found: C, 34.56; H, 2.12; N, 2.95. NMR data (in C_4D_8O): ^{1}H NMR, δ 1.33 (18 H, ^{t}Bu); ^{11}B NMR, δ –3.2; ^{13}C NMR, δ 148.7 (d, *para*, ^{1}J(CF) = 237.2 Hz), 140.3 (d, *ortho*, ^{1}J(CF) = 229.9 Hz), 137.9 (d, *meta*, ^{1}J(CF) = 250.2 Hz), 124.7 (br, ipso), 59.8 (*C*Me$_3$), 33.4 (C*Me*$_3$); ^{19}F NMR, δ –131.3 (m, *ortho*), –159.6 (s, br, *para*), –164.1 (m, *meta*); ^{125}Te NMR, δ 1682, 1672. IR (cm^{-1}): 685, 645 (Te=O). Pale yellow plate-like crystals were obtained from a THF-d_8 solution of **3** after 1 d at 23 °C. The crystals were identified as **3**·2THF by single crystal X-ray diffraction.

Preparation of (C$_6$F$_5$)$_3$B·NH$_2$^{t}Bu (4). *Tert*-butylamine (0.1 mL, 0.952 mol) was added *via* a syringe to a colorless solution of $(C_6F_5)_3B$ (0.487 g, 0.952 mmol) in *n*-pentane (30 mL) at 23 °C. The adduct **4** was formed immediately as a white solid. After 1.5 h the volatile materials were removed under vacuum to give **4** (0.462 g, 0.789 mmol, 83%). Anal. Calcd. For $C_{22}H_{11}BF_{15}N$: C, 45.16; H, 1.89; N, 2.39. Found: C, 45.17; H, 1.91; N, 2.33. NMR data (in C_7D_8): ^{1}H NMR, δ 4.36 (2 H, NH), 0.62 (9 H, ^{t}Bu); ^{11}B NMR, δ –9.0; ^{13}C NMR, δ 148.4 (d, *para*, ^{1}J(CF) = 237.8 Hz), 140.7 (d, *ortho*, ^{1}J(CF) = 287.1 Hz),

137.7 (d, *meta*, ^{1}J(CF) = 239.1 Hz), 117.0 (br, *ipso*), 57.7 (*C*Me$_3$), 28.2 (C*Me*$_3$); ^{19}F NMR, δ −131.1 (m, *ortho*), −155.1 (m, *para*), −162.2 (m, *meta*); NMR (in CD_2Cl_2): ^{1}H NMR, δ 5.11 (2 H, NH), 1.26 (9 H, ^{t}Bu); ^{11}B NMR, δ −9.0; ^{13}C NMR, δ 148.6 (d, *para*, ^{1}J(CF) = 238.5 Hz), 140.9 (d, *ortho*, ^{1}J(CF) = 251.8 Hz), 137.9 (d, *meta*, ^{1}J(CF) = 249.8 Hz), 117.8 (br, *ipso*), 59.0 (*C*Me$_3$), 29.5 (C*Me*$_3$); ^{19}F NMR, δ −132.5 (m, *ortho*), −157.0 (m, *para*), −163.4 (m, *meta*); IR (cm^{-1}): 3323, 3315, 3269, 3258 (NH). X-ray quality crystals of (**4**)$_2$·CH_2Cl_2 were obtained from the reaction of $(C_6F_5)_3B$ with $^{t}BuNH_2$ in a molar ratio 1:1 after 14 d at −20 °C.

X-ray Analyses. Crystals of **2**, **3**·2THF and (**4**)$_2$·CH_2Cl_2 were coated with Paratone oil and mounted on a CryoLoop. All measurements were made on a Nonius KappaCCD 4-Circle Kappa FR540C diffractometer using monochromated Mo K$_\alpha$ radiation (λ = 0.71073 Å) at −100 °C. Data reduction was performed with the HKL DENZO and SCALEPACK software.[18] The non-hydrogen atoms were refined anisotropically. Hydrogen atoms were included at geometrically idealized positions and were not refined. The isotropic thermal parameters of the hydrogen atoms were fixed at 1.2 times that of the preceding carbon or nitrogen atom. Neutral atom scattering factors for non-hydrogen atoms and anomalous dispersion coefficients are contained in the SHELXTL-NT 5.1 program library.[19] Crystallographic data are summarized in Table 1.

2: Yellow-orange rod (0.25 × 0.25 × 0.20 mm); 8183 reflections of the 14,360 reflections collected were independent (R_{int} = 0.0295) and 6,186 reflections were observed [$I > 2\sigma(I)$]. A multi-scan absorption correction was applied (SCALEPACK).[18] The structure was solved by direct methods (SHELXS-97)[20] and refined by full-matrix least squares method on F^2 (SHELXL97-2).[21] Two carbon atoms, labeled as C(32A), C(33A), C(32B) and C(33B), of the exocylic ^{t}Bu group were disordered over two positions with refined site occupancy factors of 0.66(1) and 0.34 (1), respectively.

3·2THF: Pale yellow plate (0.15 × 0.10 × 0.10 mm); 7925 reflections of the 14,874 reflections collected were independent (R_{int} = 0.0434), and 5,492 reflections were observed [$I > 2\sigma(I)$]. The

structure was solved by direct methods (SIR-97)[22] and refined by full-matrix least squares method on F^2 (SHELXL97-2).[21]

(4)$_2$·CH_2Cl_2: Colorless block (0.32 × 0.32 × 0.25 mm); 9,270 reflections of the 22,578 reflections collected were independent (R_{int} = 0.0782) and 7,776 reflections were observed [$I > 2\sigma(I)$]. A multi-scan absorption correction was applied. The structure was solved by direct methods (SIR-97)[22] and refined by full-matrix least squares method on F^2 (SHELXL97-2)[21] based on 9,270 reflections, 3 restraints and 730 variable parameters.

Computational Details

All molecular geometries were fully optimized with the Gaussian 98 program[23] using density functional theory. The hybrid B3PW91 functional[24,25] was chosen, since it has recently been shown to perform well in all-electron calculations for chalcogen diimides.[2,7] A mixed basis set, denoted hereafter as Gen1, was used in all optimizations. Stuttgart group's relativistic large core ECPs[26] augmented with one polarization function[27] were used for all chalcogen atoms and standard Pople-type 6-31G* basis set (as implemented in Gaussian 98) for all other elements. The fundamental frequencies were calculated to assess the nature of stationary points and to estimate the zero-point energy (ZPE) corrections.

Three different ab-initio higher-level theoretical methods were employed in the computation of accurate energetics. Single-point calculations at all optimized geometries were carried out with MP2,[28] CCSD and CCSD(T)[29] methods. Coupled cluster calculations required excessive computational resources for molecules containing four ^{t}Bu or $SiMe_3$ groups and were therefore not carried out. Single-point MP2 calculations utilizing B3PW91/Gen1 optimized geometries provide the most accurate energies that could be extended for all molecular systems reported in this work. Dunning's correlation consistent basis set of double-zeta quality, cc-pVDZ,[30] was used for all atoms except chalcogens for which ECPs with polarization functions were used as described above. This basis set combination is denoted with the abbreviation Gen2. The program package Molpro 2002.6[31] was used in all single-point energy calculations.

Results and Discussion

Preparation of [$(C_6F_5)_3B{\cdot}OTe(\mu\text{-}N^tBu)_2TeN^tBu$] (2) and [$(C_6F_5)_3B{\cdot}OTe(\mu\text{-}N^tBu)_2Te(\mu\text{-}O)]_2$ (3). Preliminary attempts to prepare the imidotelluroxane $(^tBuNTeO)_n$ by the hydrolysis of the tellurium diimide dimer $^tBuNTe(\mu\text{-}N^tBu)_2TeN^tBu$ (**1**) with water resulted in the formation of tellurium dioxide regardless of the amount of water that was used. However, the use of the hydrate $(C_6F_5)_3B{\cdot}OH_2$ as a stoichiometric reagent for this hydrolysis allowed the successive replacement of the terminal N^tBu groups in **1** by oxo ligands. Thus, the reaction of **1** with $(C_6F_5)_3B{\cdot}OH_2$ in a 1:1 molar ratio in *n*-pentane/CH_2Cl_2 produced $[(C_6F_5)_3B{\cdot}OTe(\mu\text{-}N^tBu)_2TeN^tBu]$ (**2**), which was isolated as a yellow-orange solid (Scheme 2). The subsequent reaction of **2** with an additional equivalent of $(C_6F_5)_3B{\cdot}OH_2$ in CH_2Cl_2 generated $[(C_6F_5)_3B{\cdot}OTe(\mu\text{-}N^tBu)_2Te(\mu\text{-}O)]_2$ (**3**) and the adduct $(C_6F_5)_3B{\cdot}NH_2{}^tBu$ (**4**), which was removed by washing with toluene (Scheme 2).

Insert Scheme 2 here.

Both reactions proceed in high yields (75-80%). The adduct **3** is considerably more moisture-sensitive than **2**. The attempted direct synthesis of **3** from $^tBuNTe(\mu\text{-}N^tBu)_2TeN^tBu$ and two equivalents of $(C_6F_5)_3B{\cdot}OH_2$ yielded a mixture of **2** and $(C_6F_5)_3B{\cdot}NH_2{}^tBu$ (**4**). The molecular structures of **2**, **3** and **4** were established by X-ray crystallography.

X-ray Structures of 2 and 3. The X-ray structural determination of **2** revealed that one of the terminal N^tBu groups in **1** is replaced by an oxo ligand to produce the hybrid imido-oxo system $[OTe(\mu\text{-}N^tBu)_2TeN^tBu)]$, which coordinates to the boron atom in $(C_6F_5)_3B$ via the oxygen atom (Figure 1**)**. The oxo ligand and the remaining terminal N^tBu group are in *cis* arrangement with respect to the Te_2N_2 ring. We have reported previously the formation of the imidotelluroxane $[OTe(\mu\text{-}N^tBu)_2TeN^tBu)]$, by partial hydrolysis, in the crystallization of Ag^+ and Cu^+ complexes of **1** over period of several weeks.[32] In those

complexes the terminal N^{t}Bu group is bonded to the metal and the imidotelluroxane ligand dimerizes to form a Te_2O_2 ring. The X-ray analysis of **3**·2THF showed that the second terminal N^{t}Bu group was substituted by an oxo ligand to generate the dimer [OTe(μ-N^{t}Bu)$_2$TeO], which has undergone an additional dimerization *via* O→Te interactions to give [OTe(μ-N^{t}Bu)$_2$Te(μ-O)]$_2$ (formally a tetramer of ^{t}BuNTeO), which forms the di-adduct **3** via coordination of the two terminal TeO groups to the strong Lewis acid $(C_6F_5)_3B$ (Figure 2). The oxo ligands in the tetrameric imidotelluroxane unit are in a *cis* arrangement with respect to the Te_2N_2 rings, *cf.* **2**.

The metrical parameters of **2** and **3**·2(THF) are summarized in Table 2. The Te_2N_2 ring in **2** is unsymmetrical with a mean Te–N bond length of 1.973(4) Å for the tellurium atom bonded to oxygen compared to 2.109(3) Å for the other endocyclic Te–N bonds, *cf.* ($|$d(Te-N)$|$ = 2.081(10) Å) in **1**.[9] The mean exocyclic Te–N bond length in **2** (1.865(2) Å) is comparable to that in **1** (1.876(10) Å).[10] The expected values for tellurium(IV)-nitrogen single and double bonds are 2.11 and 1.88 Å, respectively.[33] This asymmetry is more pronounced for the Te_2N_2 rings in **3** with mean Te–N bond distances of 1.960(3) and 2.050(3) Å. The longer distances involve the tellurium atom that is part of the central Te_2O_2 ring. The corresponding mean Te–N bond length in the related complex [OC(μ-N^{t}Bu)$_2$Te(μ-O)]$_2$(THF) is 2.060(2) Å.[34]

The geometry at the bridging nitrogen atoms of the Te_2N_2 rings in **2** is distorted pyramidal ($\sum\angle$[N(1)] = 348.2° and $\sum\angle$[N(2)] = 343.9°) whereas essentially planar geometry is observed for **3** ($\sum\angle$[N(1)] = 359.0° and $\sum\angle$[N(2)] = 358.9°), *cf.* 340.3° and 343.6° in **1**.[10] The torsion angle N(2)-Te(1)-N(1)-Te(2) in **2** and **3** is –5.8(2)° and 14.0(1)°, respectively, *cf.* 19.8(5)° in **1**,[10] demonstrating that the Te_2N_2 rings are less puckered than that in **1**.

The terminal Te=O bond distance in **2** (1.870(2) Å) are similar to those reported in Ag(I) and Cu(I) complexes of the same imidotelluroxane ligand.[32] The corresponding bond distance in **3** is 1.866(3) Å As found for most telluroxanes, the Te_2O_2 ring of **3** is markedly unsymmetrical with TeO distances of

1.912(3) and 2.088(3) Å [*cf.* 1.904(2) and 2.072(2) Å in $OC(\mu\text{-}N^tBu)_2Te(\mu\text{-}O)]_2(THF)$].[34] The corresponding TeO bond distances in β-TeO_2 are 1.88(2) and 1.93(2) Å.[5] The predicted Te-O single and double bond values are 2.12 and 1.89 Å, respectively.[33] Thus, to a first approximation, the Te_2O_2 ring in **3** can be viewed to involve two Te=O double bonds and two dative =O→Te bonds. The planar Te_2O_2 ring is orientated perpendicular to the two Te_2N_2 rings resulting in an overall S-shaped structure for the tetrameric imidotelluroxane ligand. Dimerization *via* O→Te interactions is prevented in **2** by the coordination of the oxygen atom to the boron atom of the $B(C_6F_5)_3$ ligand. The strength of the boron-oxygen interactions in **2** and **3** differ significantly with values of 1.657(7) Å is and 1.503(5) Å, respectively, *cf.* 1.597(2) Å in the adduct $(C_6F_5)_3B{\cdot}OH_2$.[15] This disparity suggests that, despite the comparable terminal Te=O bond lengths**,** the telluroxane ligand in **3** is a much stronger Lewis base donor towards boron than that in **2**.

The geometry at the tellurium atoms of the Te_2O_2 ring in **3** is a distorted TBP with the lone pairs on Te in a *trans* orientation with respect to each other. The equatorial bond angle O(2)-Te(2)-N(2) is 111.0(1)° and the axial bond angle N(1)-Te(2)-O(2)* is 151.6(1)°. The values for the bond angles at tellurium in the Te_2O_2 ring, 103.4(1)° at O and 76.6(1)°, are similar to those reported for related telluroxanes[32,34] and β-TeO_2.[5]

Secondary interactions between fluorine and a metal center are a common feature in borato-metal complexes, e.g., $[Cu(MeCN)_4][B(C_6F_5)_4]$[35] and $[NEt_4]_2[\{C_5H_4B(C_6F_5)_3\}Zr(\mu\text{-}Cl)Cl_2]_2$.[36] In **3** both tellurium atoms are engaged in two intramolecular Te···F interactions with contact distances of 2.948 (2), 3.080(2), 3.316(2) and 3.390(3) Å, cf. 3.53 Å for the sum of van der Waals radii for Te and F.[33] The strongest Te···F interactions involve Te(1), indicating that the charge at this atom is higher than on the second tellurium atom.[37] This tellurium atom is also involved in a Te···O secondary bonding interaction of 2.862(3) Å with the oxygen atom of a THF molecule, resulting in distorted octahedral geometry at

Te(1). Only one of the tellurium atoms, Te(1), in **2** is involved in an intramolecular Te···F interaction (3.205(2) Å).

Spectroscopic Characterization of 2 and 3. The ^{1}H NMR data for **2** in non-coordinating solvents clearly indicate the presence of two different N^{t}Bu groups in the expected ratio 1:2 (*exo*:*endo*). Interestingly, both ^{1}H and ^{13}C NMR spectra revealed the presence of two isomers **2a** and **2b** in an approximate ratio of 1.25:1 in C_7D_8 at 300 K. A variable temperature ^{1}H NMR study showed a slow conversion of **2a** into **2b** as the temperature is increased (**2a**:**2b** = 1:1.11 at 363 K}. We note that the ^{1}H and ^{13}C NMR spectra of solutions of the tellurium diimide dimer **1** in C_7D_8 also show the presence of two isomers in the approximate ratio 4:1; however, this ratio is invariant with temperature.[11,17] The ^{1}H NMR spectrum for **3** shows, as expected, only a single resonance for the N^{t}Bu groups. The ^{11}B NMR chemical shifts for **2** and **3** in C_7H_8 are observed at *ca*. –3 ppm, in the region expected for four-coordinate boron centers. The two ^{125}Te NMR resonances for the inequivalent tellurium atoms in **2 (**in CD_2Cl_2 solution) and **3** (in THF-d_8 solution) are observed at 1384, 857 ppm and at 1682, 1672 ppm, respectively, *cf*. 1480 ppm for **1** in THF-d_8 and 1553 ppm for **1**·$B(C_6F_5)_3$ in CD_2Cl_2.[38]

Spectroscopic Characterization and X-ray Structure of $(C_6F_5)_3B{\cdot}NH_2{}^{t}Bu$ (4). In order to identify the by-product **4** unambiguously, this adduct was prepared by the reaction of $(C_6F_5)_3B$ with *tert*-butylamine; it was characterized by multinuclear NMR spectroscopy and the X-ray structure was determined. Although complexes of $B(C_6F_5)_3$ with several secondary amines have been structurally characterized,[39] the adduct **4** is the first example of a primary amine adduct of tris(pentafluorophenyl)borane.[40] Nitrogen coordination to the boron center is clearly indicated by the ^{11}B NMR chemical shift of –9.0 ppm for **4,** *cf*. 59.5 and 9.0 ppm (in CD_2Cl_2) for $(C_6F_5)_3B$ and $(C_6F_5)_3B{\cdot}OH_2$, respectively. In the ^{1}H NMR spectrum the NH resonance shifts from 0.96 ppm in $^{t}BuNH_2$ (in CD_2Cl_2) to 5.10 ppm in **4**.

The asymmetric unit of $(\mathbf{4})_2{\cdot}CH_2Cl_2$ (Figure 3) consists of two molecules of **4** and one CH_2Cl_2 molecule. The two molecules differ in the orientation of the pentafluorophenyl rings. Geometrical

parameters of **4** are summarized in Table 3. The B□N bond distance of 1.633(4) Å in **4** falls within the range 1.63-1.65 Å observed for *sec*-amine adducts of $B(C_6F_5)_3$.[39a] Weak intramolecular N(H)···F contacts in the range 2.73-3.03 Å (H···F, 2.08-2.46 Å) and both intra- and intermolecular C(H)···F contacts (3.07-3.52 Å; H···F, 2.29-2.59 Å) are observed in the structure of $(\mathbf{4})_2{\cdot}CH_2Cl_2$ (see Figure 3). Similar interactions have been reported for the *sec*-amine adducts.[39] Interestingly, one of the hydrogen atoms in the NH_2 group of both molecules of **4** is involved in a bifurcated hydrogen bond.

Cyclodimerization and Cycloaddition Energies of Tellurium Diimides, Imidotelluroxanes and Related Species. In order to provide some insight into the current and previous experimental observations concerning diimides and imido-oxo derivatives of the heavy chalcogens, we have carried out quantum chemical calculations using quasi-relativistic effective core potential (ECP) basis sets for a range of derivatives. The B3PW91/Gen1 optimized geometrical parameters of chalcogen diimides $E(NR)_2$ (E = Se or Te; R = H, Me, ^{t}Bu, $SiMe_3$) and $RNTe(\mu\text{-}NR)_2TeNR$, and mixed imido-oxo systems RNTeO, $OTe(\mu\text{-}NR)_2TeNR$ and $OE(\mu\text{-}NR)_2EeO$ can be found in the Supporting Information. For all selenium derivatives the calculated geometrical parameters are in excellent agreement with previous calculations[2,7] and with experimental data for *N,N'*-diadamantyl selenium diimide $Se(NAd)_2$.[8] For tellurium compounds comparison can be made with the reported metrical parameters of ^{t}BuNTe(μ-$N^tBu)_2N^tBu$ (**1**).[10a] The calculated structural parameters for the Te_2N_2 ring are in very good agreement with experimental values; calculated and experimental endocyclic TeN bond lengths are 2.071 Å and 2.081(9) Å, respectively, and the corresponding endocyclic bond angles ∠NTeN are 75.1° and 75.6(4)°. For the exocyclic Te=N bonds, the calculated distance of 1.908 Å is slightly longer than the experimental value of 1.876(10) Å.[10a] Previous DFT calculations,[41] which did not take relativistic effects into account, predicted significantly longer endocyclic and exocyclic TeN bond lengths.

Total energies for all molecules included in this study, calculated at MP2/Gen2, CCSD/Gen2 and CCSD(T)/Gen2 levels of theory, are summarized in the Supporting Information. For monomeric selenium diimides, the *syn,anti* conformation is found to be the most stable for all derivatives except for

the parent compound $Se(NH)_2$, consistent with the X-ray structure of $Se(NAd)_2$.[8] Very recently, however, the derivative $Se(NMes^*)_2$ (Mes* = 2, 4, 6-$^tBu_3C_6H_2$) has been shown to adopt the *anti,anti* conformation in the solid state.[42] In the case of tellurium diimides, the *syn,syn* conformation is favored for $Te(NMe)_2$. Although the *syn,syn* conformation is not the energetical minimum for $Te(NR)_2$ (R = ^{t}Bu, $SiMe_3$), it is found to be very similar in energy to the *syn,anti* conformation. The *syn* conformation is also energetically favored in the case of imidotelluroxanes RNTeO. For cyclodimerization and cycloaddition products, the conformation with the lowest energy was found to be the one in which all endo- and exo-cyclic substituents are on the same side of the ENEN ring.

The gas phase [2+2] cyclodimerization energies of $E(NR)_2$ (E = S, Se, Te; R = H, Me, ^{t}Bu, $SiMe_3$) and RNTeO are summarized in Table 4 together with the cycloaddition energies of the reactions shown in Eq. 1 (E′ = S, Se) and Eq. 2.

$$E'(NR)_2 + Te(NR)_2 \rightarrow RNE'(\mu\text{-}NR)_2TeNR \quad (1)$$

$$RNTeO + Te(NR)_2 \rightarrow OTe(\mu\text{-}NR)_2TeNR \quad (2)$$

To address the question of the accuracy of the chosen computational approach, it is instructive to compare the cyclodimerization energies for selenium diimides in Table 4 with the results obtained by all-electron basis sets.[2] Although the all-electron cc-pVDZ basis set is much more flexible in the valence region than the ECP basis set, the use of ECP for chalcogens seems to have only a minor effect on cyclodimerization energies. Apparently the additional error resulting from the use of ECP basis is fairly constant and cancels out in the calculations of reaction energies. Therefore, the calculated values in Table 4 should be reasonable indicators of trends in reaction energies.

It can also be seen from Table 4 that the theoretically most reliable reaction energies, i.e. CCSD(T), fall between the MP2 and CCSD values; with some variations depending on the nature of the chalcogen. While it was not possible to carry out full CCSD and CCSD(T) calculations for all molecular systems,

these observations have been utilized to estimate semi-quantitative reaction energies at coupled cluster levels of theory when the corresponding MP2 energies are known, as shown in Figure 4.[43]

In agreement with the previous all-electron basis set calculations,[2] cyclodimerization is predicted to be approximately thermoneutral for selenium diimides, but highly exothermic for tellurium diimides consistent with the experimentally established propensity of tellurium diimides to dimerize.[10,44] The mixed-chalcogen cycloaddition reaction between sulfur and tellurium diimides (Eq. 1) is found to be approximately thermoneutral and the corresponding reaction between selenium and tellurium diimides is predicted to be an exothermic process. Consistently, preliminary experimental observations indicate that the reaction of **1** with $S(NSiMe_3)_2$ is very slow.[45]

Calculated reaction energies predict both the cyclodimerization of imidotelluroxanes RNTeO and the cycloaddition reaction of tellurium diimides and imidotelluroxanes (Eq. 2) to be highly exothermic, consistent with the experimental observations reported herein. Some general trends can gleaned from consideration of the data in Table 4: (i) both cyclodimerization and cycloaddition reactions become more exothermic when the size of the chalcogen atom increases (ii) reactions involving imido-oxo species are predicted to be more exothermic than the corresponding reactions with diimides (iii) reaction energies are nearly independent on the identity of the R group with the exception of $SiMe_3$, for which the reaction energies are constantly found to be more exothermic than for any other derivative. The reason for this anomaly is not understood.

CCSD(T)/Gen2 transition state (TS) energies were also calculated for all cyclodimerization and cycloaddition reactions involving methyl derivatives. Prior to the energy calculations, TS structures were optimized using a TS optimization algorithm and a computational method described earlier. The correct identity of each stationary point (first order saddle point) was confirmed with a subsequent frequency calculation. TS structures were only found for the cyclodimerization of selenium diimides, and for the mixed cycloaddition reaction between sulfur and tellurium diimides (see Supporting Information). All other reactions were found to proceed directly from reactants to end products. Hence,

nearly all reactions involving tellurium diimides or imidotelluroxanes are spontaneous in agreement with the experimental observation that these species are only observed as dimers or higher oligomers. Calculated activation energies for the located TSs are 39 and 37 kJ mol^{-1} for the cyclodimerization of $Se(NMe)_2$, and for the cycloaddition between $S(NMe)_2$ and $Te(NMe)_2$, respectively.

Oligomerization of Chalcogen(IV) Diimides and Imido-Oxo Systems. The formation of the tetramer $OTe(\mu\text{-}N^tBu)_2Te(\mu\text{-}O)_2Te(\mu\text{-}N^tBu)_2TeO$ in **3** can be viewed as a cyclodimerization of two $OTe(\mu\text{-}N^tBu)_2TeO$ dimers. Inevitably, this raises the question whether other chalcogen diimides or imido-oxo systems can form tetramers or, perhaps, even larger oligomers. By using the same computational approach as for the cyclodimerization reactions, we have also calculated the MP2/Gen2 reaction energies for model systems shown in Eq. 3-7. To this end, it was also necessary to optimize the structures of the tetramers formed in Eq. 3-6 and the cycloaddition product of Eq. 7. Various geometrical isomers were considered as staring points for the geometry optimization. The most stable isomer was found to be the twisted S-like structure, similar to that found for the tetrameric imidotelluroxane $OTe(\mu\text{-}N^tBu)_2Te(\mu\text{-}O)_2Te(\mu\text{-}N^tBu)_2TeO$ in **3**. The optimized geometries are listed in the Supporting Information.

$2\ OSe(\mu\text{-}NMe)_2SeO$	$\rightarrow$	$OSe(\mu\text{-}NMe)_2Se(\mu\text{-}O)_2Se(\mu\text{-}NMe)_2SeO$	(3)
$2\ OTe(\mu\text{-}NMe)_2TeO$	$\rightarrow$	$OTe(\mu\text{-}NMe)_2Te(\mu\text{-}O)_2Te(\mu\text{-}NMe)_2TeO$	(4)
$2\ MeNSe(\mu\text{-}Me)_2SeNMe$	$\rightarrow$	$MeNSe(\mu\text{-}NMe)_2Se(\mu\text{-}NMe)_2Se(\mu\text{-}NMe)_2SeNMe$	(5)
$2\ MeNTe(\mu\text{-}Me)_2TeNMe$	$\rightarrow$	$MeNTe(\mu\text{-}NMe)_2Te(\mu\text{-}NMe)_2Te(\mu\text{-}NMe)_2TeNMe$	(6)
$OSe(\mu\text{-}NMe)_2SeO +$	$\rightarrow$	$OSe(\mu\text{-}NMe)_2Se(\mu\text{-O, NMe})Te(\mu\text{-}NMe)_2TeNMe$	(7)
$MeNTe(\mu\text{-}Me)_2TeNMe$			

The calculated reaction energies in Table 5 indicate that further aggregation of $OSe(\mu\text{-}NMe)_2SeO$ (Eq. 3) is a thermoneutral process consistent with the dimeric structure observed for the *tert*-butyl

derivative.[8] In marked contrast, the reaction energy for Eq. 4 is highly exothermic in agreement with the formation of the tetrameric imidotelluroxane in **3**. The formation of the selenium diimide tetramer MeNSe(μ-NMe)$_2$Se(μ-NMe)$_2$Se(μ-NMe)$_2$SeNMe is predicted to be highly endothermic (Eq. 5) whereas the generation of the tellurium analogue (Eq. 6) is calculated to be an energetically favorable process. In practice, however, no tendency towards further aggregation has been observed for tellurium diimides, although the experimental evidence is limited to derivatives with bulky R groups.[10,44] In view of the twisted S-like structure of the model tetramer MeNTe(μ-NMe)$_2$Te(μ-NMe)$_2$Te(μ-NMe)$_2$TeNMe, it is expected that bulky R groups will greatly increase the steric hindrance involved in the formation of the tetramer. This will most likely raise the activation energy; it is also probable that it will make the overall reaction energy positive. Steric hindrance may also explain the formation of OTe(μ-N^{t}Bu)$_2$TeN^{t}Bu in **2** rather than the dimer OTe(μ-N^{t}Bu)$_2$Te(μ-N^{t}Bu)$_2$Te(μ-N^{t}Bu)$_2$TeO.

An exothermic, albeit more positive, reaction energy is also found for the formation of the mixed chalcogen system OSe(μ-NMe)$_2$Se(μ-O,□NMe)Te(μ-NMe)$_2$TeNMe suggesting that the synthesis of a mixed chalcogen system of this type is energetically feasible.

Conclusions

The terminal N^{t}Bu groups in ^{t}BuNTe(μ-N^{t}Bu)$_2$TeN^{t}Bu can be sequentially replaced by oxo via hydrolysis with $(C_6F_5)_3B{\cdot}OH_2$. The imidotelluroxanes formed in this manner coordinate through the exocyclic Te=O group to the strong Lewis acid $B(C_6F_5)_3$. This adduct formation traps the imidotelluroxane "^{t}BuNTeO" as a tetramer in which a central Te_2O_2 ring bridges two Te_2N_2 rings in an S-shaped motif.

Theoretical calculations show that the cyclodimerization of RNTeO (R = H, Me, ^{t}Bu, $SiMe_3$) and the cycloaddition of RNTeO and RNTeNR are both strongly exothermic processes. Furthermore, the calculations reveal that the association of the model dimers OE(μ-NMe)$_2$EO to give tetramers is

thermoneutral for E = Se but strongly favoured for E = Te, consistent with experimental observations. Both the experimental and theoretical investigations reported here indicate that, in the absence of a Lewis Acid acceptor to prevent further oligomerization, the imidotelluroxane ^{t}BuNTeO will form a polymer consisting of alternating Te_2O_2 and Te_2N_2 rings. The structural trend monomer $\rightarrow$ dimer $\rightarrow$ polymer for the hybrid systems ^{t}BuNEO (E = S, Se, Te) reflects the increasing reluctance of the chalcogens to form multiple bonds with oxygen (or nitrogen), which is well known for the homoleptic analogs EO_2 and $E(N^{t}Bu)_2$.

Acknowledgment. We thank Dorothy Fox, Qiao Wu, and Dr. Raghav Yamdagni for assistance in collecting NMR data and Jamie Ritch for the preparation of the adduct **4**. Financial support from the Natural Sciences and Engineering Research Council of Canada, the University of Calgary, the Academy of Finland, the Ministry of Education in Finland, and Helsingin Sanomain 100-vuotissäätiö (H.M.T.) is gratefully acknowledged.

Supporting Information Available. X-ray crystallographic information file (CIF) for **2**, **3**·2(thf) and (**4**)$_2$·CH_2Cl_2, tables of optimized geometries and absolute energies, and drawings of tetrameric and transition-state strcutures are available free of charge via the Internet at http://pubs.acs.org.

References

(1) (a) Morino, Y.; Tanimoto, M.; Saito, S. *Acta Chem. Scand., Ser. A*, **1988**, *42*, 346; (b) Buschman, J.; Steudel, W.; personal communication cited in Borrmann, T.; Lork, E.; Mews, R.; Shakirov, M. M.; Zibarev, A. V. *Eur. J. Inorg. Chem.*, **2004**, 2452.

(2) Maaninen, T.; Tuononen, H. M.; Schatte, G.; Suontamo, R.; Valkonen, J.; Laitinen, R.; Chivers, T. *Inorg. Chem.* **2004**, *43*, 2097.

(3) Stahl, K.; Legros, J.-P.; Galy, J. *Z. Kristallogr.* **1992**, *202*, 99.

(4) Two new (metastable) phases of SeO_2 have been reported recently. Orosel, D.; Leynaud, O.; Balog, P; Jansen, M. *Solid State Chem.*, **2004**, *177*, 1631.

(5) (a) Lindqvist, O. *Acta. Chem. Scand.*, **1968**, *22*, 977; (b) Beyer, H. *Z. Kristallogr.*, **1967**, *124*, 228; (c) Champarnaud-Mesjard, J. C.; Blanchadin, S.; Thomas, P.; Mitgorodsky, A.; Merle-Mejean, T.; Frit, B.; *J. Phys. Chem. Solids*, **2000**, *61*, 1499.

(6) Ozin, G. A.; Vander Voet, A. *J. Mol. Struct.*, **1971**, *10*, 173.

(7) Tuononen, H. M.; Suontamo, R. J.; Valkonen, J.; Laitinen, R. S.; Chivers, T. *Inorg. Chem.* **2003**, *42*, 2447, and references cited therein.

(8) Maaninen, T.; Laitinen, R.; Chivers, T. *Chem. Commun.* **2002**, 1812.

(9) Chivers, T.; Gao, X.; Parvez, M. *J. Chem. Soc., Chem. Commun.* **1994**, 2149.

(10) Chivers, T.; Gao, X.; Parvez, M. *J. Am. Chem. Soc.* **1995**, *117*, 2359.

(11) Chivers, T.; Gao, X.; Parvez, M. *Inorg. Chem.* **1996**, *35*, 9.

(12) (a) Herberhold, M.; Distler, B.; Maisel, H.; Milius, W.; Wrackmeyer, B.; Zanello, P. *Z. Anorg. Allg. Chem.* **1996**, *622*, 1515; (b) Vrieze, K.; van Koten, G. *J. R. Netherlands Chem. Soc.* **1980**, *99*, 145.

(13) (a) Kirchoff, W. H. *J. Am. Chem. Soc.* **1969**, *91*, 2437; (b) Beagly, B.; Chantrell, S. J.; Kirby, R. G.; Schmidling, D. G. *J. Mol. Struct.* **1975**, *25*, 319.

(14) Herberhold, M; Jellen, W. *Z. Naturforsch.*, **1986**, *41B*, 144.

(15) Doerrer, L. H.; Green, M. L. H. *J. Chem. Soc., Dalton Trans.* **1999**, 4325.

(16) Neculai, D.; Roesky, H. W.; Neculai, A. M.; Magull, J.; Walfort, B.; Stalke, D. *Angew. Chem. Int. Ed. Engl*. **2002**, *41*, 4294.

(17) Chivers, T.; Sandblom, N.; Schatte, G. *Inorg. Synth.* **2004**, *34*, 42.

(18) *HKL DENZO* and *SCALEPACK* v1.96: Otwinowski, Z.; Minor, W. *Processing of X-ray Diffraction Data Collected in Oscillation Mode, Methods in Enzymology, Vol. 276*: *Macromolecular Crystallography*; Carter, C. W., Jr., Sweet, R. M., Eds.; Academic Press: San Diego, CA, 1997; pp. 307-326.

(19) *SHELXTL-NT 5.1*: *Program Library for Structure Solution and Molecular Graphics*; Bruker AXS, Inc.: Madison, WI, 1998.

(20) Sheldrick, G. M. *SHELXS-97*: *Program for the Solution of Crystal Structures*; University of Göttingen: Göttingen, Germany 1997.

(21) Sheldrick, G. M. *SHELXL97-2*: *Program for the Solution of Crystal Structures*; University of Göttingen: Göttingen, Germany 1997.

(22) Altomare, A.; Cascarano, G.; Giacovazzo, C.; Guagliardi, A.; Moliterni, A. G. G.; Burla, M.C.; Polidori, G.; Camalli, M.; Spagna, R. *SIR-97*: *A Package for Crystal Structure Solution by Direct Methods and Refinement*. *J. Appl. Crystallogr*. **1999**, *32*, 115.

(23) Frisch, M.J.; Trucks; G.W.; Schlegel, H.B.; Scuseria, G.E.; Robb, M.A.; Cheeseman, J.R.; Zakrzewski, V.G.; Montgomery, J.A Jr.; Stratmann, R.E.; Burant, J.C.; Dapprich, S.; Millam, J.M.; Daniels, A.D.; Kudin, K.N.; Strain, M.C.; Farkas, O.; Tomasi, J.; Barone, V.; Cossi, M.; Cammi, R.; Mennucci, B.; Pomelli, C.; Adamo, C.; Clifford, S.; Ochterski, J.; Petersson, G.A.; Ayala, P.Y.; Cui, Q.; Morokuma, K.; Salvador, P.; Dannenberg, J.J.; Malick, D.K.; Rabuck, A.D.; Raghavachari, K.; Foresman, J.B.; Cioslowski, J.; Ortiz, J.V.; Baboul, A.G.; Stefanov, B.B.; Liu, G.; Liashenko, A.; Piskorz, P.; Komaromi, I.; Gomperts, R.; Martin, R.L.; Fox, D.J.; Keith, D.J.; Al-Laham, M.A.; Peng, C.Y.; Nanayakkara, A.; Challacombe, M.; Gill, P.M.W.; Johnson, B.; Chen, B.; Wong, M.W.; Andres, J.L.; Gonzalez, C.; Head-Gordon, M.; Replogle, E.S.; Pople, J.A., Gaussian 98 (Revision A.11), Gaussian, Inc., Pittsburgh PA, 2001.

(24) Becke, A.D. *J. Chem. Phys.* **1993**, *98*, 5648.

(25) Perdew, J.P.; Wang, Y. *Phys. Rev. B* **1992**, *45*, 13244.

(26) The Stuttgart ECP basis sets were used as presented in the EMSL basis set library. http://www.emsl.pnl.gov/forms/basisform.html

(27) Huzinaga, S., Ed.; *Gaussian Basis Sets for Molecular Calculations*, *Physical Science data 16*; Elsevier: Amsterdam, 1984, pp. 23-25.

(28) M□ller, C.; Plesset, M.S. *Phys. Rev.* **1934**, *46*, 618.

(29) See, for example, Bartlett, R.J. *J. Phys. Chem.* **1989**, *93*, 1697, and references therein.

(30) The cc-pVDZ basis set was used as it referenced in the Molpro 2002.6 internal basis set library.

(31) MOLPRO is a package of ab initio programs designed by Werner, H.-J. and Knowles, P.J. The authors are Amos, R.D.; Bernhardsson, A.; Berning, A.; Celani, P.; Cooper, D.L.; Deegan, M.J.O.; Dobbyn, A.J.; Eckert, F.; Hampel, C.; Hetzer, G.; Knowles, P.J.; Korona, T.; Lindh, R.; Lloyd, A.W.; McNicholas, S.J.; Manby, F.R.; Meyer, W.; Mura, M.E.; Nicklaß, A.; Palmieri, P.; Pitzer, R.; Rauhut, G.; Schütz, M.; Schumann, U.; Stoll, H.; Stone A. J.; Tarroni, R.; Thorsteinsson, T.; Werner, H.-J..

(32) Chivers, T.; Parvez, M.; Schatte, G. *Inorg. Chem.* **1999**, *38*, 5171.

(33) Pauling, L. *The Nature of the Chemical Bond*, 3rd Edn. Cornell University Press, Ithaca, NY, 1960.

(34) Schatte, G.; Chivers, T.; Jaska, C.; Sandblom, N. *Chem. Comm.* **2000**, 1657.

(35) Liang, H.-C.; Kim, E.; Incarvito, C. D.; Rheingold, A. L.; Karlin, K. D. *Inorg. Chem.* **2002**, *41*, 2209.

(36) Lancaster, S. J.; Thornton-Pett, M.; Dawson, D. M.; Bochmann, M. *Organometallics* **1998**, *17*, 3829.

(37) Alcock, N. W. *Adv. Inorg. Chem. Radiochem.* **1972**, *15*, 1.

(38) Chivers, T.; Schatte, G. *Eur. J. Inorg. Chem.* **2003**, 3314.

(39) (a) Mountford, A. J.; Hughes, D. L.; Lancaster, S. J. *Chem. Commun.* **2003**, 2148; (b) Dunitz, J. D.; Taylor, R. *Chem. Eur. J.*, **1997**, *3*, 89.

(40) Piers, W. *Adv. Organomet. Chem.*, **2004**, *52*, in press.

(41) Sandblom, N.; Ziegler, T.; Chivers, T. *Inorg. Chem.*, **1998**, *37*, 354.

(42) Maaninen, T.; Tuononen, H. M.; Kosunen, K.; Oulunkaniemi, R.; Hiitola, J.; Laitinen, R.; Chivers, T. *Z. Anorg. Allg. Chem*., **2004**, *630*, 1947.

(43) By considering energy values of the molecules that could be calculated at all three correlated levels, the semi-quantitative contributions of one sulfur, selenium and tellurium atom to the correction of the reaction energies could be established. It can be seen from Figure 4 that these contributions establish reasonable estimates for the CCSD/Gen2//B3PW91/Gen1 and CCSD(T)/Gen2//B3PW91/Gen1 reaction energies, when the corresponding MP2/Gen2//B3PW91/Gen1 energy values are known (see also ref. 2)

(44) Chivers, T.; Gao, X.; Parvez, M. *J. Chem. Soc., Chem. Commun.* **1994**, 2149.

(45) Sandblom, N.; Chivers, T. unpublished results.

Table 1. Crystallographic Data for **2**, **3**·2(THF) and (**4**)$_2$·CH_2Cl_2

	2	**3**·2(THF)	(**4**)$_2$·CH_2Cl_2
formula	$C_{30}H_{27}BF_{15}N_3OTe_2$	$C_{60}H_{52}B_2F_{30}N_4O_6Te_4$	$C_{45}H_{24}B_2Cl_2F_{30}N_2$
fw	996.56	2027.08	1255.18
space group	*P*2$_1$/*n* (No. 14)	*P*2$_1$/*n* (No. 14)	*P*1 (No. 1)
a, Å	16.5310(2)	15.0520(3)	10.6217(2)
b, Å	13.0060(2)	15.6130(3)	10.6283(2)
c, Å	18.0770(2)	15.5230(4)	10.8588(2)
α, deg	90	90	83.6308(8)
β, deg	112.4910(8)	105.5280(10)	88.2839(8)
γ, deg	90	90	76.1307(9)
V, Å^3	3590.98(8)	3514.86(13)	1182.76(4)
Z	4	2	1
T, °C	-100	-100	-100
λ, Å	0.71073	0.71073	0.71073
d_{calcd}, g cm^{-3}	1.843	1.915	1.762
λ, cm^{-1}	17.32	17.75	2.95
F(000)	1920	1952	622
R_1[a]	0.0306	0.0363	0.0448
wR_2[b]	0.0702	0.0837	0.1155

[a] $R_1 = [\Sigma||F_o|-|F_c||]/[\Sigma|F_o|]$ for $[I > 2\sigma(I)]$.

[b] $wR_2 = \{[\Sigma w(F_o^2-F_c^2)^2]/[\Sigma w(F_o^2)^2]\}^{1/2}$ (all data).

Table 2. Selected Bond Lengths (Å) and Bond Angles (°) for **2** and **3**·2(THF)[a]

	2	**3**·2(THF)
Te(1)-N(1)	1.968(2)	1.942(3)
Te(1)-N(2)	1.979(2)	1.978(3)
Te(1)-O(1)	1.870(2)	1.866(3)
Te(2)-N(1)	2.104(2)	2.079(3)
Te(2)-N(2)	2.114(2)	2.022(3)
Te(2)-N(3)	1.865(2)	-
Te(2)-O(2)	-	1.912(3)
Te(2)-O(2)*	-	2.088(3)
O(1)-B(1)	1.515(4)	1.503(5)
N(1)-C(10)	1.494(4)	1.488(5)
N(2)-C(20)	1.503(4)	1.504(5)
N(3)-C(30)	1.496(4)	-
C(41)-B(1) / C(31)-B(1)	1.646(4)	1.635(6)
C(51)-B(1) / C(41)-B(1)	1.661(4)	1.659(6)
C(61)-B(1) / C(51)-B(1)	1.662(4)	1.648(6)
O(1)-Te(1)-N(1)	97.58(9)	97.9(1)
O(1)-Te(1)-N(2)	99.25(9)	97.2(1)
O(2)-Te(1)-N(1)	-	88.4(1)
O(2)-Te(1)-N(2)	-	110.0(1)
O(2)-Te(2)-O(2)*	-	76.6(1)
N(1)-Te(1)-O(2)*	-	151.6(1)
N(2)-Te(1)-O(2)*	-	88.7(1)
N(1)-Te(1)-N(2)	79.56(9)	78.3(1)
N(1)-Te(2)-N(2)	73.56(9)	74.3(1)
N(3)-Te(2)-N(1) / O(2)-Te(2)-N(1)	110.8(1)	88.4(1)
N(3)-Te(2)-N(2) / O(2)-Te(2)-N(2)	110.0(1)	111.0(1)
Te(1)-N(1)-Te(2)	102.2(1)	103.1(1)
Te(1)-N(2)-Te(2)	101.5(1)	103.9(1)
Te(2)-O(2)-Te(2)*	-	103.4(1)
B(1)-O(1)-Te(1)	127.6(2)	147.2(2)
C(10)-N(1)-Te(1)	123.0(2)	126.5(2)
C(10)-N(1)-Te(2)	123.1(2)	129.4(2)
C(20)-N(2)-Te(1)	121.8(2)	126.1(2)
C(20)-N(2)-Te(2)	120.7(2)	128.9(2)
C(30)-N(3)-Te(2)	131.0(2)	-

[a] Symmetry transformations used to generate equivalent atoms: * $-x, -y + 1, -z + 1$.

Table 3. Selected Bond Lengths (Å) and Bond Angles (°) for (**4**)$_2$·CH_2Cl_2[a]

First Molecule	
N(1)-B(1)	1.633(4)
N(1)-C(10)	1.557(4)
C(31)-B(1)	1.641(4)
C(41)-B(1)	1.640(4)
C(51)-B(1)	1.669(4)
C(10)-N(1)-B(1)	126.3(2)
C(32)-C(31)-B(1)	127.8(3)
C(36)-C(31)-B(1)	118.7(3)
C(42)-C(41)-B(1)	127.1(3)
C(46)-C(41)-B(1)	119.5(3)
C(52)-C(51)-B(1)	126.5(2)
C(56)-C(51)-B(1)	119.9(3)
N(1)-B(1)-C(31)	106.3(2)
N(1)-B(1)-C(41)	111.7(2)
N(1)-B(1)-C(51)	106.8(2)

[a] There are two molecules of **4** in the asymmetric unit. The bond distances and bond angles for the second molecule are essentially identical to those observed for the first molecule.

Table 4. Cyclodimerization and Cycloaddition Energies of Chalcogen Diimides and Hybrid Imido-Oxo Species (kJ mol^{-1})[a]

Reaction	H	Me	^{t}Bu	$SiMe_3$
2RNSeNR → RNSe(μ-NR)$_2$SeNR				
MP2/Gen2	43	30	47	–11
CCSD/Gen2	8	–3	–	–
CCSD(T)/Gen2	25	11	–	–
2RNTeNR → RNTe(μ-NR)$_2$TeNR				
MP2/Gen2	–61	–47	–47	–123
CCSD/Gen2	–118	–116	–	–
CCSD(T)/Gen2	–85	–82	–	–
RNSNR + RNTeNR → RNS(μ-NR)$_2$TeNR				
MP2/Gen2	45	24	36	–23
CCSD/Gen2	–11	–17	–	–
CCSD(T)/Gen2	10	3	–	–
RNSeNR + RNTeNR → RNSe(μ-NR)$_2$TeNR				
MP2/Gen2	0	–8	1	–66
CCSD/Gen2	–54	–59	–	–
CCSD(T)/Gen2	–29	–35	–	–
2RNTeO → OTe(μ-NR)$_2$TeO				
MP2/Gen2	–128	–123	–131	–160
CCSD/Gen2	–169	–153	–	–
CCSD(T)/Gen2	–135	–130	–	–
RNTeO + RNTeNR → OTe(μ-NR)$_2$TeNR				
MP2/Gen2	–97	–90	–96	–143
CCSD/Gen2	–145	–139	–	–
CCSD(T)/Gen2	–112	–105	–	–

[a] Values include unscaled zero point energy corrections.

Table 5. Cyclodimerization and Cycloaddition Energies of Chalcogen Diimide Dimers and Imido-Oxo Dimers (kJ mol^{-1})[a]

Reaction			**Energy**
2 OSe(μ-NMe)$_2$SeO	$\rightarrow$	OSe(μ-NMe)$_2$Se(μ-O)$_2$Se(μ-NMe)$_2$SeO	0
2 OTe(μ-NMe)$_2$TeO	$\rightarrow$	OTe(μ-NMe)$_2$Te(μ-O)$_2$Te(μ-NMe)$_2$TeO	–188
2 MeNSe(μ-NMe)$_2$SeNMe	$\rightarrow$	MeNSe(μ-NMe)$_2$Se(μ-NMe)$_2$Se(μ-NMe)$_2$SeNMe	+656
2 MeNTe(μ-NMe)$_2$TeNMe	$\rightarrow$	MeNTe(μ-NMe)$_2$Te(μ-NMe)$_2$Te(μ-NMe)$_2$TeNMe	–190
OSe(μ-NMe)$_2$SeO + MeNTe(μ-NMe)$_2$TeNMe	$\rightarrow$	OSe(μ-NMe)$_2$Se(μ-O,NMe)Te(μ-NMe)$_2$TeNMe	–77

[a] At MP2/Gen2//B3PW91/Gen1 level of theory. Values include unscaled zero point energy corrections.

Captions for Figures

Figure 1. Molecular structure of **2**. Thermal ellipsoids are shown at 50% probability level. Only one disordered pair [C(32A) and C(33A)] is shown. Hydrogen atoms are omitted for clarity.

Figure 2. Molecular structure of **3.** Thermal ellipsoids are shown at 50% probability level. Hydrogen atoms are omitted for clarity.

Figure 3. Molecular structure of **4** indicating the hydrogen-bonding network linking the molecules. Thermal ellipsoids are shown at 50% probability level.

Figure 4. Trends in cyclodimerization and cycloaddition reaction energies at different levels of theory.

○ Reaction energies calculated at MP2/Gen2//B3PW91/Gen1 level of theory.

□ Reaction energies calculated at CCSD/Gen2//B3PW91/Gen1 level of theory.

△ Reaction energies calculated at CCSD(T)/Gen2 /B3PW91/Gen1 level of theory.

□ △ Estimates based on the trends calculated by the above-mentioned MP2, CCSD, and CCSD(T) calculations.

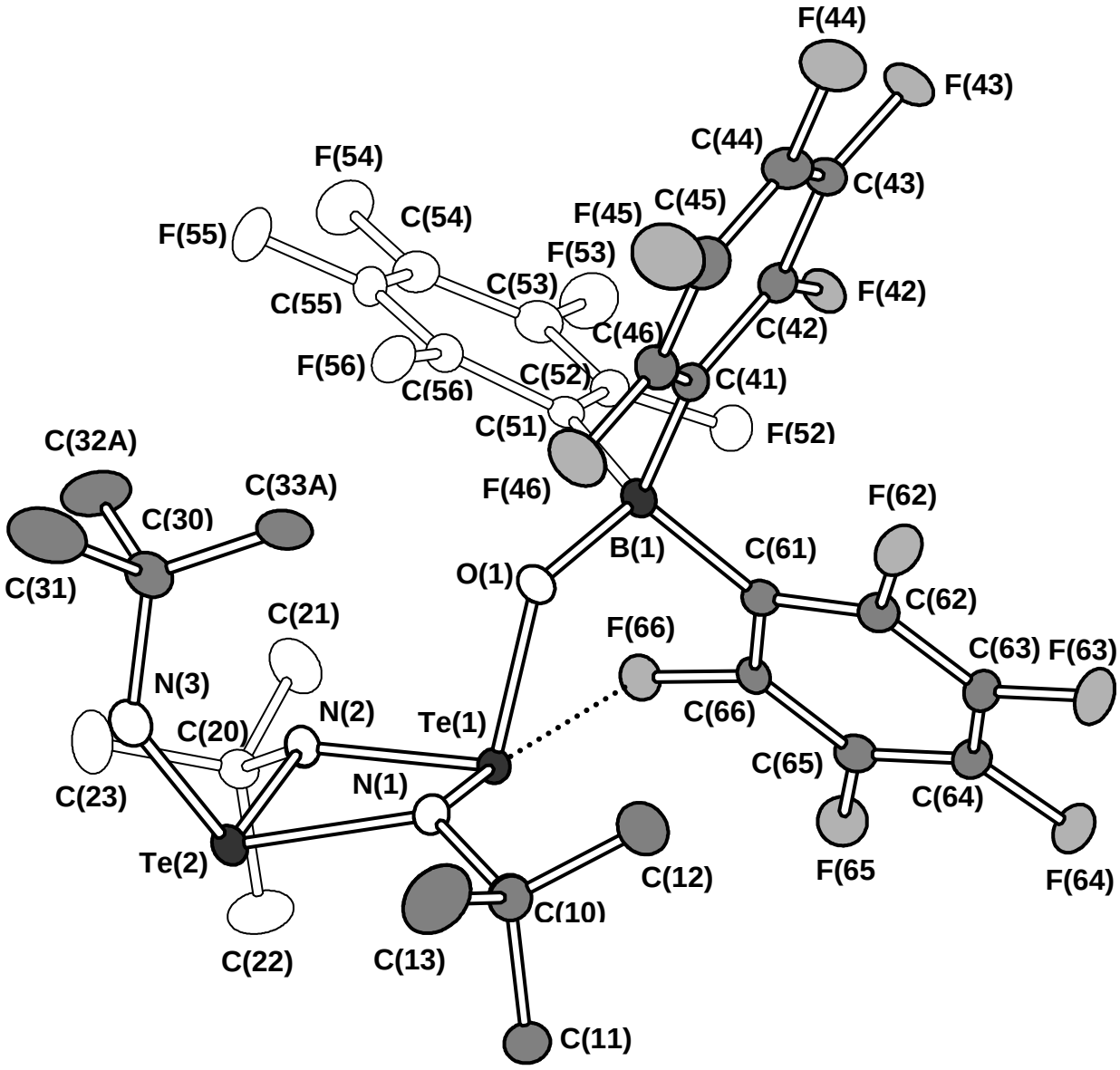
F(44)
F(43)
C(44)
C(43)
F(54)
C(54)
F(55)
F(45)
C(45)
F(53)
C(53)
C(55)
F(42)
C(46)
C(42)
F(56)
C(56)
C(52)
C(41)
C(51)
F(52)
C(32A)
C(33A)
F(46)
F(62)
C(30)
B(1)
C(61)
C(31)
O(1)
C(62)
C(21)
F(66)
C(63)
F(63)
N(3)
N(2)
C(66)
C(20)
Te(1)
C(65)
C(23)
N(1)
C(64)
Te(2)
F(65
C(12)
F(64)
C(10)
C(22)
C(13)
C(11)

Figure 1.

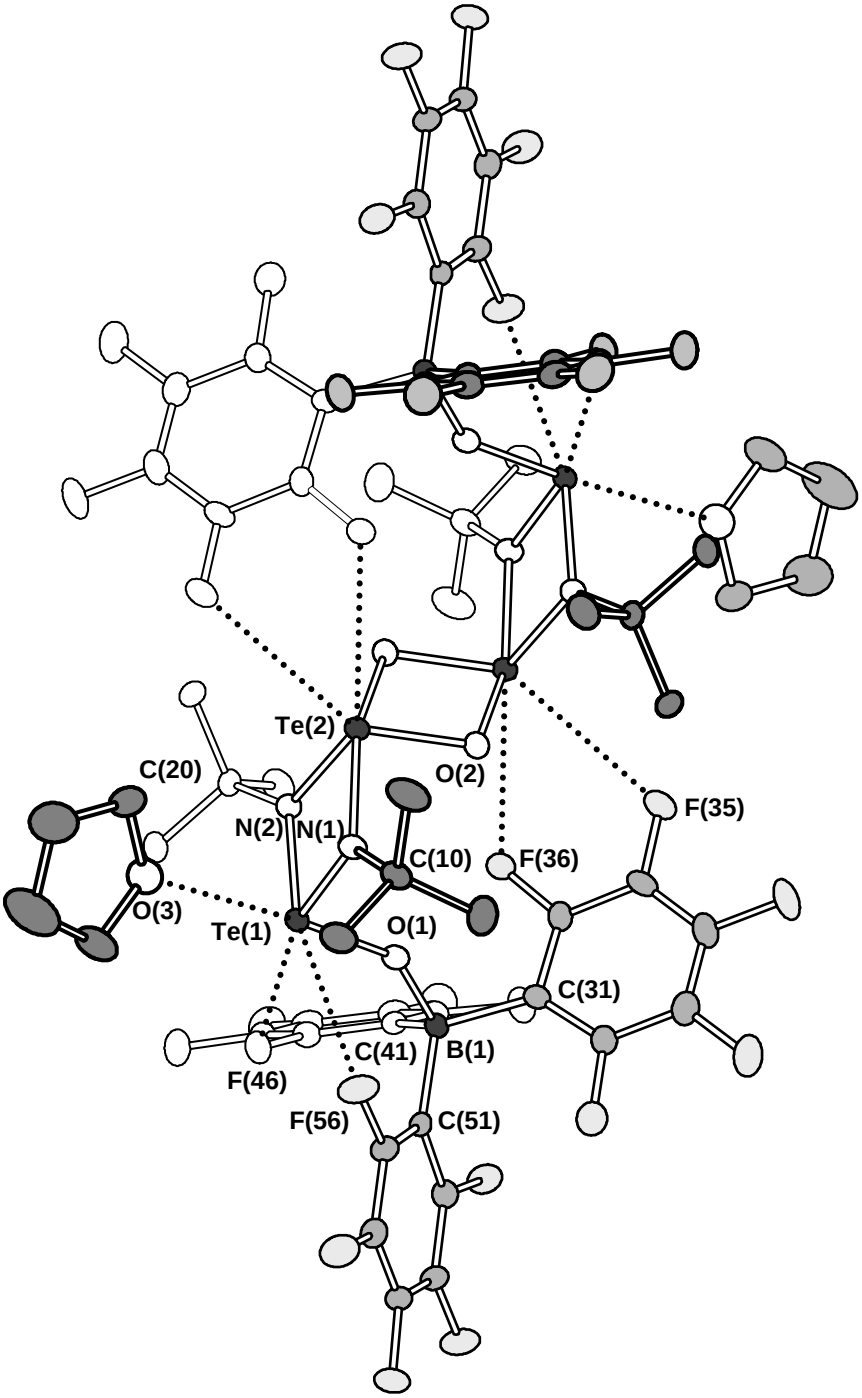

Figure 2.

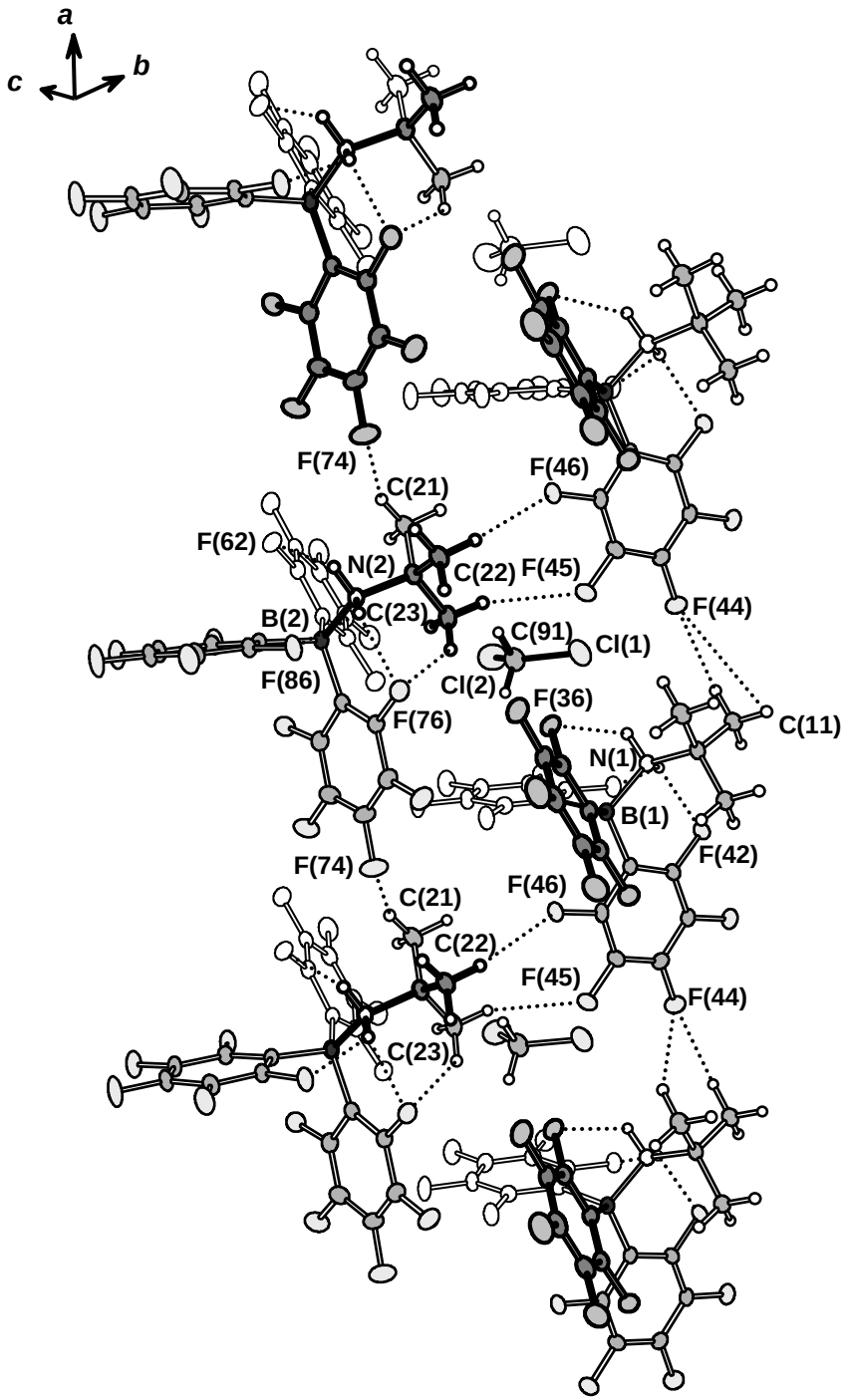
a
b
c
F(74)
C(21)
F(46)
F(62)
N(2)
C(22)
F(45)
B(2)
C(23)
F(44)
C(91)
Cl(1)
F(86)
Cl(2)
F(36)
F(76)
C(11)
N(1)
B(1)
F(42)
F(74)
C(21)
F(46)
C(22)
F(45)
F(44)
C(23)

Figure 3.

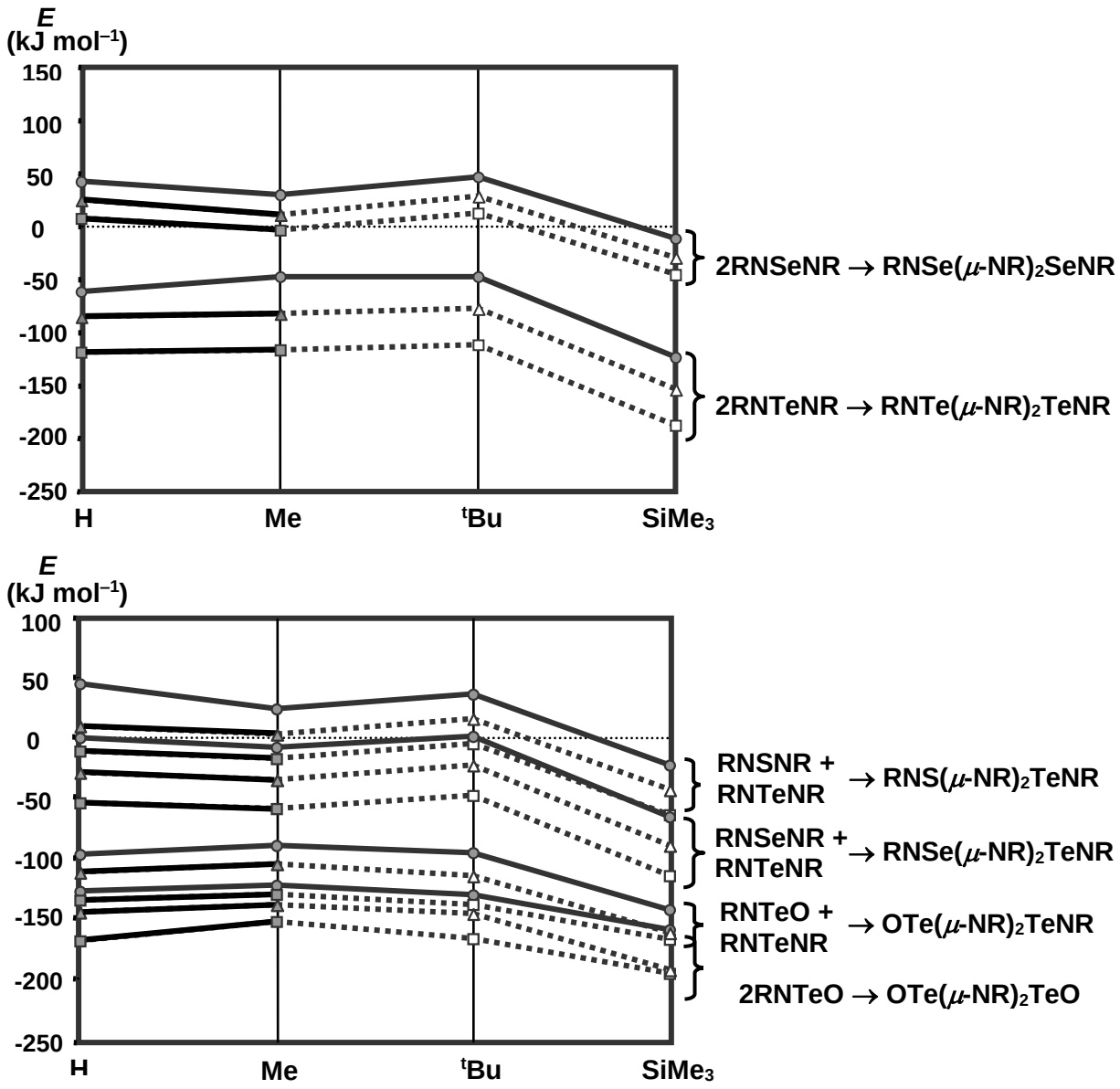
E
(kJ mol–1)
150
100
50
0
-50
-100
-150
-200
-250
H
Me
tBu
SiMe3
2RNSeNR → RNSe(μ-NR)2SeNR
2RNTeNR → RNTe(μ-NR)2TeNR
E
(kJ mol–1)
100
50
0
-50
-100
-150
-200
-250
H
Me
tBu
SiMe3
RNSNR + RNTeNR → RNS(μ-NR)2TeNR
RNSeNR + RNTeNR → RNSe(μ-NR)2TeNR
RNTeO + RNTeNR → OTe(μ-NR)2TeNR
2RNTeO → OTe(μ-NR)2TeO

Figure 4.

Scheme 1

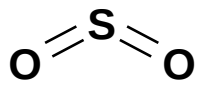

monomeric gas

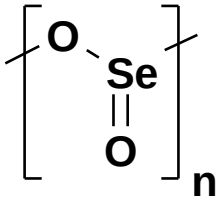

2-D polymer

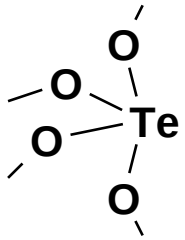

3-D polymer

Scheme 2